Dynamics of Flexible Multibody Systems with Non-Holonomic Constraints: A Finite Element Approach

A.L. SCHWAB and J.P. MEIJAARD[★]
Laboratory for Engineering Mechanics, Delft University of Technology, Mekelweg 2,
2628 CD Delft, The Netherlands

Abstract. In this article it is shown how non-holonomic constraints can be included in the formulation of the dynamic equations of flexible multibody systems. The equations are given in state space form with the degrees of freedom, their derivatives and the kinematic coordinates as state variables, which circumvents the use of Lagrangian multipliers. With these independent state variables for the system the derivation of the linearized equations of motion is straightforward. The incorporation of the method in a finite element based program for flexible multibody systems is discussed. The method is illustrated by three examples, which show, among other things, how the linearized equations can be used to analyse the stability of a nominal steady motion.

Key words: non-holonomic constraints, flexible multibody systems, linearized equations of motion, finite element method, general purpose software.

1. Introduction

The motion of mechanical systems having rolling contact, as in road vehicles and track-guided vehicles, can be investigated in an approximate way by a mechanical model having non-holonomic constraints. These constraints express the conditions of vanishing slips at the contact points. A mechanical system with non-holonomic constraints is called non-holonomic. Whereas the dynamics of mechanical systems with ideal holonomic constraints was almost completed by the publication of Lagrange's monumental *Méchanique analitique* [1], Hertz [2] was the first to describe and name systems with non-holonomic constraints. Although the principle of minimal action fails for these systems, the principle of virtual power and the principle of D'Alembert can be applied. In their excellent book [3] Neĭmark and Fufaev treat the kinematics and dynamics of non-holonomic mechanical systems in great detail. They illustrate the presented theory with worked-out examples and give an elaborate reference list with 513 items. The inclusion of non-holonomic constraints in formalisms for multibody systems has been considered by Kreuzer [4] and

---

[★] Present address: School of Mechanical, Materials, Manufacturing Engineering and Management, University of Nottingham, University Park, Nottingham NG7 2RD, England, U.K.

Nikravesh [5], and by such they made the first step from small-scale analytically manipulated problems to general purpose software.

In this article we present a procedure for including non-holonomic constraints in the formulation of the dynamical equations of flexible multibody systems. The method is incorporated in a finite element based program. The dynamical equations are given for a set of minimal coordinates rather than with the aid of Lagrangian multipliers. The configuration is described by the degrees of freedom and the generalized kinematic coordinates, as many as there are non-holonomic constraints. The velocities of the system are described by the time derivatives of the degrees of freedom. The dynamical equations in a state space form comprise the equations of motion and the kinematic differential equations, which give the time derivatives of the configuration coordinates.

The derivation of the linearized equations from the dynamical equations is rather straightforward. These linearized equations can be used to analyse small vibrations superimposed on a general rigid body motion as described in [6]. Here we will extend that idea and use the linearized equations to analyse the stability of a nominal steady motion, as will be shown in some examples.

2. Dynamics of Non-Holonomic Flexible Multibody Systems

2.1. FINITE ELEMENT MODELLING

Multibody systems with deformable bodies may well be modelled by finite elements. This approach was initiated in the seventies by Besseling [7] and has been further developed among others by Van der Werff [8], Jonker [9], Géradin and Cardona [10, 11], and authors [12, 13]. The distinguishing point in the finite element approach as it has been developed in Delft and implemented in the program SPACAR [14] is the specification of independent deformation modes of the finite elements, the so-called generalized deformations or generalized strains. These are the algebraic analogue to the continuous field description of deformations. Rigid body motions are displacements for which the generalized strains are zero. If the specification of the generalized strains remains valid for arbitrarily large translations and rotations, rigid multibody systems such as mechanisms and machines can be analysed by setting all generalized strains to zero. These strain equations are now the constraint equations which express rigidity. Deformable bodies are handled by allowing non-zero strains and specifying constitutive equations for the generalized stresses, which are the duals of the generalized strains.

Instead of imposing constraint equations for the interconnection of bodies, which is a widespread approach in multibody system dynamics formalisms, permanent contact of elements is achieved by letting them have nodal points in common. With the help of a rather limited number of element types it is possible to model a wide class of systems. Typical types of elements are beam, truss and hinge elements, while more specialized elements can be used to model joint con-

nections, transmissions of motion [18], and rolling contact as in road vehicles and track-guided vehicles [19, 20].

2.2. HOLONOMIC AND NON-HOLONOMIC CONSTRAINTS

In a finite element description of a multibody system the configuration is described by a number of nodal points with coordinates $\mathbf{x}$ and a number of elements with generalized deformations or generalized strains $\boldsymbol{\varepsilon}$. The nodal coordinates can be absolute coordinates of the position or parameters that describe the orientation of the nodes, such as Euler parameters. The generalized deformations depend on the nodal coordinates and can be expressed as

$$\boldsymbol{\varepsilon} = \mathbf{D}(\mathbf{x}). \tag{1}$$

Usually holonomic constraints are imposed on some generalized deformations and nodal coordinates. For instance, the conditions for rigidity of element e are $\boldsymbol{\varepsilon}^e = \mathbf{D}^e(\mathbf{x}^e) = \mathbf{0}$. If the holonomic constraints are consistent, the coordinates can locally be expressed as functions of the generalized coordinates $\mathbf{q}$ by means of a transfer function $\mathbf{F}$ as

$$\mathbf{x} = \mathbf{F}(\mathbf{q}, t). \tag{2}$$

The prescribed motions, or rheonomic constraints, which are known explicit functions of time, are represented here by the time t. The generalized coordinates can be chosen from components of the nodal coordinate vector $\mathbf{x}$ and the generalized deformation vector $\boldsymbol{\varepsilon}$. Generally the transfer function cannot be calculated explicitly, but has to be determined by solving the constraint equations numerically in an iterative way. Partial derivatives are calculated by means of implicit differentiation.

The non-holonomic constraints, as may arise from elements having idealized rolling contact, can be expressed in terms of slips that are zero [19]. Such a slip is usually defined as some relative velocity between the two bodies in the contact area, and is therefore linear in the velocities. The case of non-linear non-holonomic constraints in mechanical systems has been given a lot of attention in the past [3] but only led to one example system as originally given by Appell in 1911. Hence we will consider only linear non-holonomic constraints expressed in terms of zero slip functions. For instance, if element e has non-slipping contacts, it has to satisfy the constraints $\mathbf{s}^e = \mathbf{V}^e(\mathbf{x}^e)\dot{\mathbf{x}}^e = \mathbf{0}$. Assembly of all conditions of zero slip for the system results in the non-holonomic constraints

$$\mathbf{s} = \mathbf{V}(\mathbf{x})\dot{\mathbf{x}} = \mathbf{0}. \tag{3}$$

Owing to these constraints, the generalized velocities $\dot{\mathbf{q}}$ are now dependent. This dependency is expressed by a splitting of the generalized coordinates $\mathbf{q}$ into the degrees of freedom $\mathbf{q}^d$ and the generalized kinematic coordinates $\mathbf{q}^k$. The velocities of the degrees of freedom $\dot{\mathbf{q}}^d$ are now the independent speeds, whereas the configuration of the system is described by $\mathbf{q}^d$ and $\mathbf{q}^k$. The velocities of the system can

now be expressed in terms of the first-order transfer function $\mathbf{H}$ times the velocities of the degrees of freedom and a term representing the prescribed motion, as in

$$\dot{\mathbf{x}} = \mathbf{H}(\mathbf{q}, t)\dot{\mathbf{q}}^d + \mathbf{v}(\mathbf{q}, t). \tag{4}$$

The expressions for the first-order transfer function and the prescribed motion terms are found by differentation of (2) and splitting of terms as in

$$\dot{\mathbf{x}} = \mathbf{F}_{,\mathbf{q}^d}\dot{\mathbf{q}}^d + \mathbf{F}_{,\mathbf{q}^k}\dot{\mathbf{q}}^k + \mathbf{F}_{,t}, \tag{5}$$

where partial derivatives are denoted by a subscript comma followed by the variable. Substitution in the non-holonomic constraints (3) results in

$$\mathbf{V}[\mathbf{F}_{,\mathbf{q}^d}\dot{\mathbf{q}}^d + \mathbf{F}_{,\mathbf{q}^k}\dot{\mathbf{q}}^k + \mathbf{F}_{,t}] = \mathbf{0}. \tag{6}$$

From these equations, as many as there are kinematic coordinates $\mathbf{q}^k$, the velocities $\dot{\mathbf{q}}^k$ can be solved as

$$\dot{\mathbf{q}}^k = -(\mathbf{V}\mathbf{F}_{,\mathbf{q}^k})^{-1}[\mathbf{V}\mathbf{F}_{,\mathbf{q}^d}\dot{\mathbf{q}}^d + \mathbf{V}\mathbf{F}_{,t}]. \tag{7}$$

Substitution of this result in (5) and comparing terms with (4) results in the first-order transfer function

$$\mathbf{H} = [\mathbf{I} - \mathbf{F}_{,\mathbf{q}^k}(\mathbf{V}\mathbf{F}_{,\mathbf{q}^k})^{-1}\mathbf{V}]\mathbf{F}_{,\mathbf{q}^d}, \tag{8}$$

and the velocities $\mathbf{v}$, representing the prescribed motion, as

$$\mathbf{v} = [\mathbf{I} - \mathbf{F}_{,\mathbf{q}^k}(\mathbf{V}\mathbf{F}_{,\mathbf{q}^k})^{-1}\mathbf{V}]\mathbf{F}_{,t}. \tag{9}$$

The expresion between square brackets that is common to (8) and (9) is a projection operator to the space $\mathbf{V}\dot{\mathbf{x}} = \mathbf{0}$ in a direction that is parallel to the space spanned by the columns of $\mathbf{F}_{,\mathbf{q}^k}$. In this expression we identify the use of the inverse of the Jacobian of the non-holonomic constraints with respect to the generalized kinematic coordinates

$$\mathbf{V}\mathbf{F}_{,\mathbf{q}^k}. \tag{10}$$

If this Jacobian is singular, we have to choose another set of generalized kinematic coordinates and consequently another set of degrees of freedom to describe the system uniquely. Having taken into account all constraints we can define the state of the system at a time t as

$$(\dot{\mathbf{q}}^d, \mathbf{q}^d, \mathbf{q}^k). \tag{11}$$

Next we will derive the dynamical equations of the system, or, in other words, the time derivative of the state of the system.

2.3. EQUATIONS OF MOTION

The derivative of the first part of the state vector, $\dot{\mathbf{q}}^d$, with respect to time follows from the equations of motion of the system. The equations of motion for the constraint multibody system will be derived from the principle of virtual power and the principle of D'Alembert. This method can be traced back to Lagrange who by his monumental *Méchanique analitique* [1] became the founder of the study of motion of systems of bodies. The inclusion of non-holonomic constraints was not foreseen by Lagrange. Hertz [2] was the first to describe and this type of constraints.

First, for each node and element in the system, we determine a mass matrix $\mathbf{M}^e$ and a force vector $\mathbf{f}^e$, which give a contribution to the virtual power of

$$\delta\dot{\mathbf{x}}^{eT}(\mathbf{f}^e - \mathbf{M}^e\ddot{\mathbf{x}}^e). \tag{12}$$

The virtual power equation of the system is obtained by assembling the contribution of all elements and nodes in a global mass matrix $\mathbf{M}$ and a global force vector $\mathbf{f}$, which results in

$$\delta\dot{\mathbf{x}}^T[\mathbf{f}(\dot{\mathbf{x}}, \mathbf{x}, t) - \mathbf{M}(\mathbf{x})\ddot{\mathbf{x}}] = 0. \tag{13}$$

Here, $\delta\dot{\mathbf{x}}$ are kinematically admissible virtual velocities, which satisfy all instantaneous kinematic constraints. They follow directly from (4) as

$$\delta\dot{\mathbf{x}} = \mathbf{H}\delta\dot{\mathbf{q}}^d. \tag{14}$$

The coordinate accelerations are obtained by differentation of the velocities (4), resulting in

$$\ddot{\mathbf{x}} = \mathbf{H}(\mathbf{q}, t)\ddot{\mathbf{q}}^d + \mathbf{g}(\dot{\mathbf{q}}, \mathbf{q}, t), \tag{15}$$

where we have collected all convective and prescribed accelerations in $\mathbf{g}$. These accelerations, which depend only on the state of the system, are given by

$$\mathbf{g} = \mathbf{H}_{,\mathbf{q}}\dot{\mathbf{q}}\dot{\mathbf{q}}^d + \mathbf{H}_{,t}\dot{\mathbf{q}}^d + \mathbf{v}_{,\mathbf{q}}\dot{\mathbf{q}} + \mathbf{v}_{,t}. \tag{16}$$

Substitution of the acceleration (15) in the virtual power equation (13) yields the reduced equations of motion

$$\bar{\mathbf{M}}(\mathbf{q}^d, \mathbf{q}^k, t)\ddot{\mathbf{q}}^d = \bar{\mathbf{f}}(\dot{\mathbf{q}}^d, \mathbf{q}^d, \mathbf{q}^k, t), \tag{17}$$

with the reduced global mass matrix,

$$\bar{\mathbf{M}} = \mathbf{H}^T\mathbf{M}\mathbf{H}, \tag{18}$$

and the reduced global force vector,

$$\bar{\mathbf{f}} = \mathbf{H}^T[\mathbf{f} - \mathbf{M}\mathbf{g}]. \tag{19}$$

The time derivative of the second part of the state vector, $\mathbf{q}^d$, is obviously the first part of the state vector itself. The time derivative of the generalized kinematic coordinates, $\mathbf{q}^k$, as found in (7), can in general be expressed as

$$\dot{\mathbf{q}}^k = \mathbf{A}(\mathbf{q}, t)\dot{\mathbf{q}}^d + \mathbf{b}(\mathbf{q}, t), \tag{20}$$

where the matrix $\mathbf{A}$ and the velocity vector $\mathbf{b}$, which represents the velocities of the rheonomic constraints, are given by

$$\mathbf{A} = -(\mathbf{VF}_{,\mathbf{q}^k})^{-1}\mathbf{VF}_{,\mathbf{q}^d} \quad \text{and} \quad \mathbf{b} = -(\mathbf{VF}_{,\mathbf{q}^k})^{-1}\mathbf{VF}_{,t}. \tag{21}$$

Note in both expressions the presence of the inverse of the Jacobian (10).

We summarize by writing down the time derivative of the state vector or the state equations as

$$\frac{\mathrm{d}}{\mathrm{d}t}\begin{bmatrix} \dot{\mathbf{q}}^d \\ \mathbf{q}^d \\ \mathbf{q}^k \end{bmatrix} = \begin{bmatrix} \bar{\mathbf{M}}^{-1}\bar{\mathbf{f}} \\ \dot{\mathbf{q}}^d \\ \mathbf{A}\dot{\mathbf{q}}^d + \mathbf{b} \end{bmatrix}. \tag{22}$$

2.4. LINEARIZED EQUATIONS OF MOTION

The study of small vibrations and stability of conservative non-holonomic systems near equilibrium states has lead to some controversy in the past. Whittaker in his *Analytical Dynamics* [15, section 90] concluded that for such cases 'the difference between holonomic and non-holonomic systems is unimportant' and that the vibration motion of a given non-holonomic system with n independent coordinates and m non-holonomic constraints is the same as that of a certain holonomic system with $n - m$ degrees of freedom. Bottema [16] showed that this was incorrect, and pointed out that the characteristic determinant of such a non-holonomic system is asymmetric and that the corresponding characteristic equation possesses as many vanishing roots as there are non-holonomic constraints. However, besides a manifold of equilibrium states, some non-holonomic systems also possess a manifold of steady motion. Due to these motions some vanishing roots may get non-zero values.

To describe the small vibrations or motions with respect to a nominal steady motion we have to linearize the dynamical equations (22). Whereas in the nominal motion the rolling contacts satisfy the non-holonomic zero-slip conditions, the small vibrations may violate some of these conditions. Small slips are usually allowed in contact models for road and railway vehicles. For the description of the small motions we will use the dynamic degrees of freedom $\mathbf{q}^d$. The linearization is done in the nominal reference state which is characterized by $(\dot{\mathbf{q}}^d, \mathbf{q}^d, \mathbf{q}^k) = (\mathbf{0}, \mathbf{0}, \mathbf{q}_0^k)$, where $\mathbf{q}_0^k$ stands for the kinematic coordinates in the reference state. Linearization of the first part of the state equations (22), the reduced equations of motion (17), results in

$$\bar{\mathbf{M}}\Delta\ddot{\mathbf{q}}^d + \bar{\mathbf{C}}\Delta\dot{\mathbf{q}}^d + \bar{\mathbf{K}}^d\Delta\mathbf{q}^d + \bar{\mathbf{K}}^k\Delta\mathbf{q}^k = -\mathbf{f}^d, \tag{23}$$

where the prefix Δ denotes a small increment. $\bar{\mathbf{M}}$ is the reduced mass matrix as in (18), $\bar{\mathbf{C}}$ is the velocity sensitivity matrix which contains terms resulting from damping and gyroscopic effects, $\bar{\mathbf{K}}^d$ and $\bar{\mathbf{K}}^k$ are the total stiffness matrices. Note the extra term $\bar{\mathbf{K}}^k \Delta \mathbf{q}^k$ which is due to the variation of the kinematic coordinates $\mathbf{q}^k$. The forcing, $-\mathbf{f}^d$, on right-hand side of the equations results from the nominal steady motion solution. In order to maintain the prescribed values for the dynamic degrees of freedom and the kinematic coordinates during this motion, usually additional forces have to be introduced in the right-hand side of the reduced equations of motion (17). The sum of the reduced forces has to be zero, as in

$$\mathbf{H}^T[\mathbf{f} - \mathbf{Mg}] + \mathbf{f}^d = \mathbf{0}, \tag{24}$$

from which the forces $\mathbf{f}^d$ are found.

The matrices of the linearized equations are determined in the following way. First for all elements and nodes the contribution to the global stiffness matrix $\mathbf{K}$ and the global velocity matrix $\mathbf{C}$ are determined as

$$\mathbf{C}^e = -(\mathbf{f}^e)_{,\dot{\mathbf{x}}^e} \quad \text{and} \quad \mathbf{K}^e = (\mathbf{M}^e \ddot{\mathbf{x}}^e - \mathbf{f}^e)_{,\mathbf{x}^e}. \tag{25}$$

These global matrices having been determined, the matrices in the linearized equations are given by

$$\bar{\mathbf{C}} = \mathbf{H}^T \mathbf{C} \mathbf{H} + \mathbf{H}^T \mathbf{Mg}_{,\dot{\mathbf{q}}^d},$$
$$\bar{\mathbf{K}} = [\bar{\mathbf{K}}^d \ \bar{\mathbf{K}}^k] = \mathbf{H}^T \mathbf{K} \mathbf{F}_{,\mathbf{q}} + \mathbf{H}_{,\mathbf{q}}^T [\mathbf{M}\ddot{\mathbf{x}} - \mathbf{f}] + \mathbf{H}^T [\mathbf{Mg}_{,\mathbf{q}} + \mathbf{Cv}_{,\mathbf{q}}]. \tag{26}$$

Note that all matrices are generally a function of time due to the non-linear steady motion. Linearization of the second part of Equation (22) is trivial. The last part, the linearization of the rate of the generalized kinematic coordinates is derived from (20) as

$$\Delta \dot{\mathbf{q}}^k = \mathbf{A}(\mathbf{q}, t) \Delta \dot{\mathbf{q}}^d + \mathbf{B}^d(\mathbf{q}, t) \Delta \mathbf{q}^d + \mathbf{B}^k(\mathbf{q}, t) \Delta \mathbf{q}^k. \tag{27}$$

The $\mathbf{B}$-matrices express the sensitivity of the generalized kinematic velocities with respect to the generalized coordinates, and are given by

$$\mathbf{B}^d(\mathbf{q}, t) = \mathbf{b}_{,\mathbf{q}^d} \quad \text{and} \quad \mathbf{B}^k(\mathbf{q}, t) = \mathbf{b}_{,\mathbf{q}^k} \tag{28}$$

We conclude by summarizing the linearization of the state equations in matrix vector form as

$$\begin{bmatrix} \bar{\mathbf{M}} & \mathbf{0} & \mathbf{0} \\ \mathbf{0} & \mathbf{I} & \mathbf{0} \\ \mathbf{0} & \mathbf{0} & \mathbf{I} \end{bmatrix} \begin{bmatrix} \Delta \ddot{\mathbf{q}}^d \\ \Delta \dot{\mathbf{q}}^d \\ \Delta \dot{\mathbf{q}}^k \end{bmatrix} + \begin{bmatrix} \bar{\mathbf{C}} & \bar{\mathbf{K}}^d & \bar{\mathbf{K}}^k \\ -\mathbf{I} & \mathbf{0} & \mathbf{0} \\ -\mathbf{A} & -\mathbf{B}^d & -\mathbf{B}^k \end{bmatrix} \begin{bmatrix} \Delta \dot{\mathbf{q}}^d \\ \Delta \mathbf{q}^d \\ \Delta \mathbf{q}^k \end{bmatrix} = \begin{bmatrix} -\mathbf{f}^d \\ \mathbf{0} \\ \mathbf{0} \end{bmatrix}. \tag{29}$$

The stability of a system in steady motion can be investigated by the homogeneous linearized state equation from (29). Under the usual assumption of an exponential motion with respect to time for the small variations $(\Delta \dot{\mathbf{q}}^d, \Delta \mathbf{q}^d, \Delta \mathbf{q}^k)^T$ we end
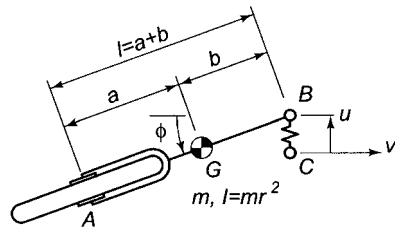
Figure 1. Swivel wheel.

up with a characteristic equation for the unknown exponents. The stability of an equilibrium state, the case of zero steady motion as investigated by Bottema [16], corresponds to vanishing **B**-matrices. Because there is now a manifold of equilibria with the same dimension as the number of non-holonomic constraints, there are as many vanishing roots as there are non-holonomic constraints. These roots entail eigenvectors with $\Delta \mathbf{q}^k$ the individual unit vectors, $\Delta \mathbf{q}^d = -(\bar{\mathbf{K}}^d)^{-1}\bar{\mathbf{K}}^k \Delta \mathbf{q}^k$ and $\Delta \dot{\mathbf{q}}^d = \mathbf{0}$.

3. Examples

3.1. SWIVEL WHEEL SHIMMY

To illustrate the general method for the derivation of the state equations of a non-holonomic system and their linearization we shall revisit the shimmy problem of an aircraft landing gear as treated by Den Hartog [17]. He simplified the problem in order to show the principal mechanism responsible for the shimmy phenomenon. The mass and stiffness of the airplane are assumed large with respect to those of the swivel landing wheel, so that the attachment point of the swivel axis to the airplane may be assumed to move forward at a constant speed. The tire is assumed to be rigid and the inertia along the axis of rotation of the wheel is not taken into account. Then in Figure 1, which is a plan view of the shimmying wheel seen from above, point C is the point where the wheel strut is built into the airplane. Point B is the bottom point of the strut; normally B is right under C, but while shimmying the strut is assumed to flex sideways through distance u at a stiffness k. The wheel is behind B with angle ϕ, the shimmy angle, which is zero for normal ideal operation. A is the centre of the wheel, and G is the centre of gravity of the combined landing gear. The finite element model consists of a two-dimensional wheel element [19] attached in point A to a rigid beam. The wheel has zero lateral slip which is the non-holonomic condition in the system. The beam is connected in point B to a cylindrical bearing element. The bearing is rigid in the longitudinal and flexible in the lateral and rotational direction and the generalized deformations are denoted by u and ϕ. The lateral stiffness is k while the rotational stiffness is assumed to be zero. The bearing is moved forward with a constant speed of v. The generalized coordinates of the system are given by $\mathbf{q} = (u, \phi)$. The zero lateral slip

condition on the wheel reduces the coordinates to the degree of freedom $\mathbf{q}^d = (u)$ and the kinematic coordinate $\mathbf{q}^k = (\phi)$. The steady state undeformed motion is characterized by $(\dot{u}, u, \phi) = (0, 0, 0)$. With the variations $\Delta \dot{\mathbf{q}}^d = \Delta \dot{u}$, $\Delta \mathbf{q}^d = \Delta u$ and $\Delta \mathbf{q}^k = \Delta \phi$, the coefficients of the linearized state derivatives according to (29) are

$$\bar{\mathbf{M}} = m \left(\frac{a^2 + r^2}{l^2} \right),$$

$$\bar{\mathbf{C}} = m \left(\frac{ab - r^2}{l^2} \right) \frac{v}{l}, \quad \mathbf{A} = \frac{1}{l},$$

$$\bar{\mathbf{K}}^d = k, \quad \mathbf{B}^d = 0,$$

$$\bar{\mathbf{K}}^k = -m \left(\frac{ab - r^2}{l^2} \right) \frac{v^2}{l}, \quad \mathbf{B}^k = -\frac{v}{l},$$

$$\bar{\mathbf{f}} = 0. \tag{30}$$

These coefficients are usually numerically calculated by the program but we present them here in an analytical form so we can compare them with the approach as presented by Den Hartog [17]. His *ad hoc* analysis leads to an eigenvalue problem. The systematically derived linearized state derivatives (30) lead to the same eigenvalue problem and consequently to the same prediction of unstable shimmy behaviour.

To investigate the shimmy motion we start with the usual assumption of an exponential motion for the small variations $\Delta \mathbf{q}$ of the form $\Delta \mathbf{q}_0 \exp(\lambda t)$. The characteristic equation of the eigenvalue problem from (29) with the coefficients from (30) is

$$\lambda^3 + (1 + \mu)\omega \lambda^2 + \omega_n^2 \lambda + \omega \omega_n^2 = 0, \tag{31}$$

with the mass distribution factor $\mu = (ab - r^2)/(a^2 + r^2)$, the driving frequency $\omega = v/l$ and the natural frequency $\omega_n = \sqrt{kl^2/(m(a^2 + r^2))}$. A neccessary and sufficient condition for asymptotic stability is given by the requirement that all roots of (31) have negative real parts. Application of Hurwitz's theorem on the characteristic equation (31) yields

$$\omega > 0 \quad \text{and} \quad \mu > 0. \tag{32}$$

In other words, the motion is stable if the driving speed v is positive and the centre of mass is positioned such that $a(l - a) > r^2$. The latter corresponds to a region of $\pm\sqrt{(l/2)^2 - r^2}$ around the midpoint $a = l/2$. For the critical case, where $a(l-a) = r^2$, there is one real eigenvalue $\lambda_1 = -\omega$ describing the non-oscillating decaying motion and a pair of conjugated imaginary values $\lambda_{2,3} = \pm\omega_n i$ which describe the undamped oscillatory solution. This critical case corresponds to a mass distribution where point B is the centre of percussion or in other words, the lateral contact force in A has no influence on the lateral spring force in B.
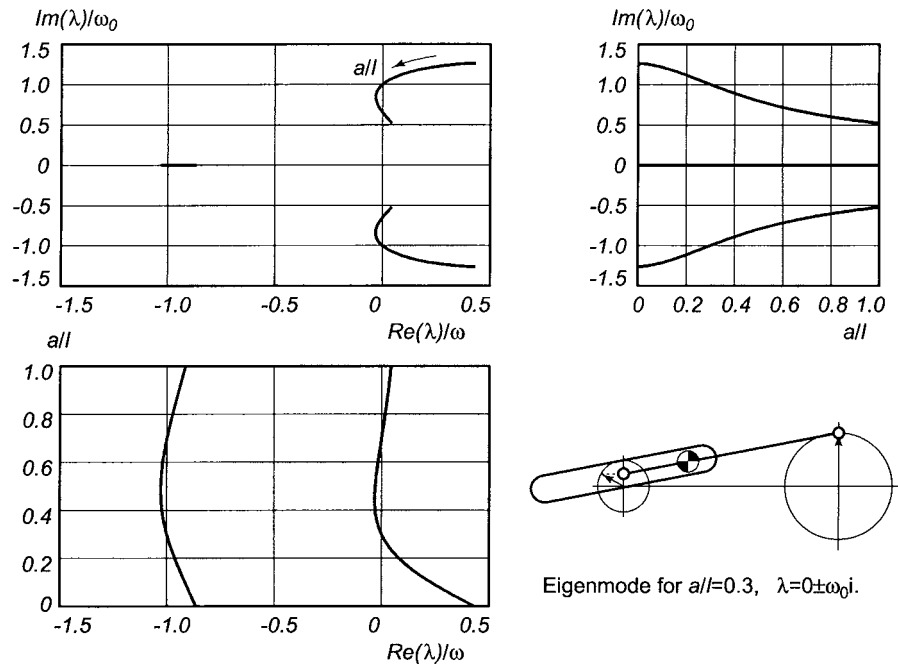
Figure 2. Root loci of the eigenvalues λ for the swivel wheel with moment of inertia $I = 0.21ml^2$ in the centre of mass position range of $0 \le a/l \le 1$ and eigenmode for the undamped oscillatory case $a/l = 0.3$, with driving frequency $\omega = v/l$ and undamped eigenfrequency $\omega_0 = \sqrt{k/(0.3m)}$.

The general solution for the eigenvalues can be found by solving the characteristic equation (31). However, the general solution of a cubic equation leads to lengthy expressions and gives little insight in the nature of the solution. To illustrate the behaviour of the system at the non-critical cases, consider a swivel wheel with mass moment of inertia $I = 0.21ml^2$. The motion is stable if the centre of mass position a is between $0.3l$ and $0.7l$. The root loci for this example in range of $0 \le a/l \le 1$ are shown in Figure 2 together with the eigenmode for the undamped oscillatory case $a/l = 0.3$. The lateral displacement of the attachment point B, u, and the lateral displacement of the centre of the wheel A, denoted by w, are illustrated in the figure by the vertical projection of the rotating arrows. Note that the lateral displacements are not in phase. The phase angle, ψ, and the amplitude ratio, $\Delta w_0/\Delta u_0$, are for given eigenvalue $\lambda = \gamma_0 + \omega_0 i$ uniquely determined by the kinematic rate equation (27) and read

$$\tan \psi = -\frac{\omega_0}{\omega + \gamma_0} \quad \text{and} \quad \frac{\Delta w_0}{\Delta u_0} = \frac{\omega}{\sqrt{(\omega + \gamma_0)^2 + \omega_0^2}}. \tag{33}$$

The wheel centre and the attachment point are always out of phase, even in the undamped oscillatory case where $\gamma_0 = 0$.
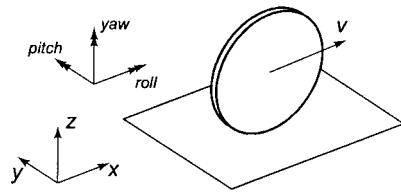
Figure 3. Disk rolling on a horizontal plane.
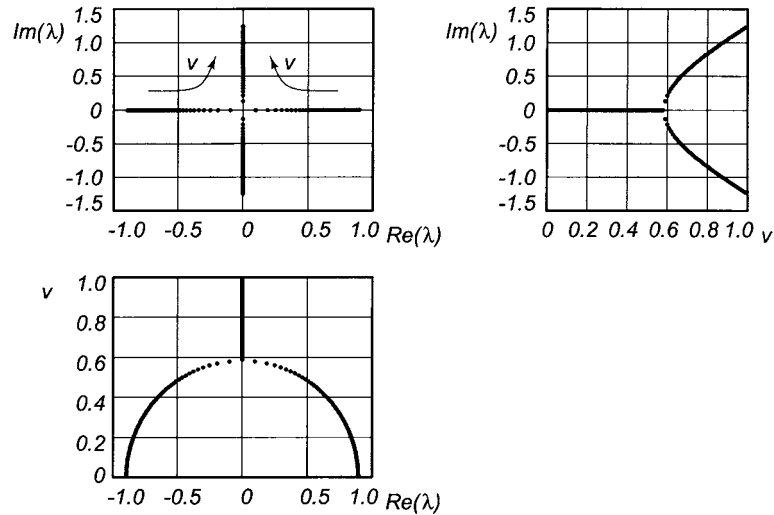
Figure 4. Root loci of the eigenvalues λ for the rectilinear motion of a rolling disk on a horizontal plane in the speed range of $0 \le v \le 1$.

3.2. THE ROLLING DISK

One of the simplest and most intriguing examples of a spatial non-holonomic system is a disk rolling without slip on a horizontal plane. From experience we know that such an object, if given enough initial speed, shows stable motion which is quite different from the behaviour at low speed. We shall investigate the stability of the rectilinear motion with the help of the spatial wheel element [19]. The rolling of a disk on a horizontal plane has been studied in detail, for example by Neĭmark and Fufaev [3], and we shall compare the results. The finite element model of the system consists of a wheel element, rolling on a horizontal plane $z = 0$, and three orthogonal hinges attached to the wheel centre to describe the three degrees of freedom: pitch, roll and yaw (Figure 3). The two kinematic coordinates are the x and y position of the point of contact in the plane. We assume that the infinitesimally thin disk has uniformly distributed unit mass m, unit radius r and a unit gravitational force field g in the downward direction.

The stability of the rectilinear motion at longitudinal speed v is investigated by the determination of the eigenvalues of the linearized equations of motion as de-
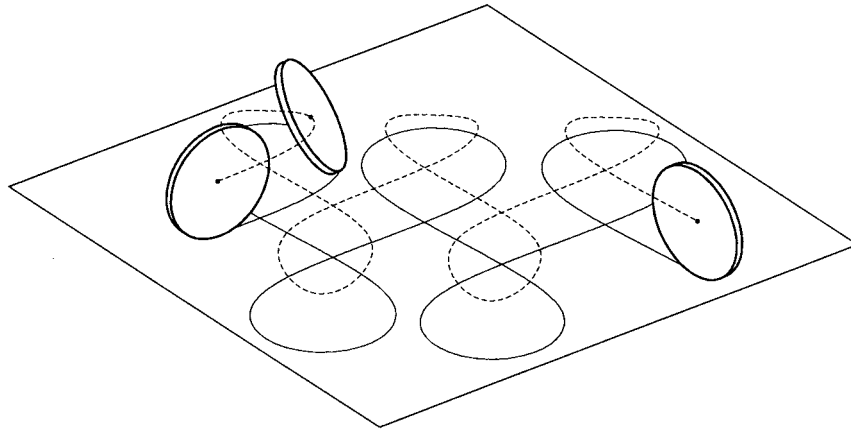
Figure 5. Path of a rolling disk on a horizontal plane at subcritical speed for a time period of 87 units, with an initial forward velocity 0.4116 and a roll velocity −0.01.

scribed in Section 2.4 by Equation (29). The dimension of the eigenvalue problem is eight; namely two times the number of degrees of freedom plus the number of kinematic coordinates. Beforehand we know that there are six zero eigenvalues. The first two pairs are a consequence of the two cyclic coordinates, the pitch and the yaw, in the system. The potential energy is only a function of the rotation along the longitudinal axis, the roll angle. The last two zero eigenvalues describe the kinematic motion of the point of contact (x, y). The remaining two non-zero eigenvalues of the perturbed rectilinear motion in the speed range of $0 \leq v \leq 1$, where speed scales according to $\sqrt{gr}$, are shown in Figure 4. At low speed there are two equal and opposite real eigenvalues describing unstable perturbed motion, just like an inverted pendulum. At increasing speed these eigenvalues move to zero, where at the critical speed [3], $v = 1/\sqrt{3} \approx 0.58$, they change into a pair of conjugated imaginary values which describe an undamped oscillatory motion. The corresponding eigenmode is of the slalom type and can best be characterised by a 90° phase angle between the roll and the yaw motion. Further increase of the speed shows an approximately linear increase in the eigenvalues.

The unstable perturbed motion, below the critical speed, is illustrated by a transient analysis. The initial conditions are a vertical position with a forward speed of $v = 0.4116$, an angular roll velocity of −0.01 and a zero yaw rate. The path of the centre of the disk and the path of the contact point in the plane are shown in Figure 5 for the time period of 87 units, where one time unit scales according to $\sqrt{r/g}$. The low roll velocity starts the initially exponentially increasing inclination of the disk, after which it makes a sharp turn and rises up again to the vertical position. This motion is repeated at equal time intervals and in alternating turning directions. The unstable rectilinear motion is transformed into a quasi periodic motion where the disk continues to wobble forward. The initial conditions were chosen such that the
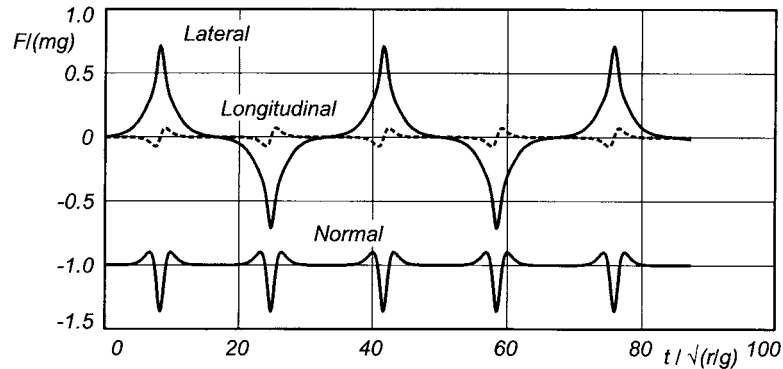
Figure 6. Forces in the contact point of a rolling disk on a horizontal plane at subcritical speed for a time period of 87 units, with an initial forward velocity 0.4116 and a roll velocity −0.01.

path shows a nice geometric figure where the contact point intersects itself almost perpendicular.

The forces in the contact point exerted by the wheel on the plane for this quasi periodic motion are shown in Figure 6. During cornering the lateral and normal force increase in magnitude whereas the longitudinal contact force shows a short oscillation indicating an accelerating and decelerating longitudinal motion. The ratio of the in-plane contact force to the normal contact force during cornering is at most 0.52. The friction coefficient must be above this value to ensure rolling without slipping.

However, if we assume that the rolling contact is not ideal and the tangential contact forces are linear functions of the slip velocities, then the disk on a smooth surface will slip into an almost cyclic motion during the first turn. In this motion the centre of mass mainly moves in the downward direction while the rotation of the point of contact increases rapidly. The disk will eventually come to the singular horizontal rest position in a finite time. Compare this to the behaviour of the contemporary executive toy known as 'Euler's Disk'; a smooth edged disk on a slight concave supporting bowl which whirrs and shudders to a horizontal rest.

3.3. KINEMATIC SHIMMY OF A CASTER WHEEL

As an example of a flexible multibody system with non-holonomic constraints we will analyse the kinematic (or static) shimmy of a caster wheel of an aircraft landing gear. Kantrowitz [21] was the first who analysed this kinematic shimmy and demonstrated the phenomena in an experimental setup. The mass of the airplane is assumed large with respect to the caster wheel assembly, so that the attachment point of the yoke to the airplane may be assumed to move forward at a constant speed v. Then in Figure 7, which is a back view and side view of the assembly, point B is the point where the yoke is hinged to the airplane. To demonstrate the principal mechanism for the kinematic shimmy we will assume that the caster length (trail)
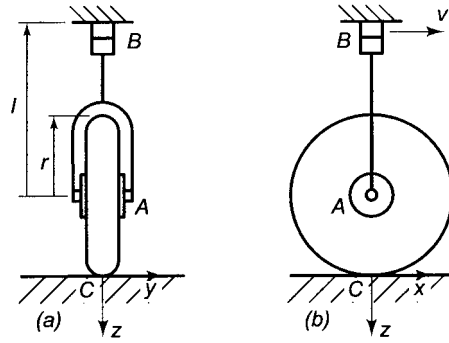
Figure 7. Caster wheel moving at a forward speed v; (a) back view and (b) side view.

and the caster angle (rake angle) are zero, resulting in the wheel centre A and the contact point C of the wheel vertically under B. For the wheel-surface contact we will assume a finite contact area with zero longitudinal slip, zero lateral slip, and zero spin; these are the three non-holonomic conditions on the system. The yoke A–B is assumed to have a finite bending stiffness such that point A can flex sideways and that the wheel axle can rotate along he x-axis, the roll angle. To make the problem statically determinate we release the radial deflection of the tire.

In a first approximation we assume the lateral deflection in A to be negligible. This model has zero degrees of freedom but due to the three non-holonomic constraints, it has three kinematic coordinates. For these kinematic coordinates we choose the three successive rotations of the wheel, starting with a yaw angle ψ along the global z-axis followed by the roll angle ϕ along the rotated x-axis and finally the pitch angle θ along the wheel local y-axis. These three coordinates define the state of the system. In the absence of the degrees of freedom $\mathbf{q}^d$ the linearized state equations (29) now only have the $\mathbf{B}^k$ matrix term, reading

$$
\begin{bmatrix} \Delta\dot{\psi} \\ \Delta\dot{\phi} \\ \Delta\dot{\theta} \end{bmatrix} = \begin{bmatrix} 0 & \omega & 0 \\ -\omega & 0 & 0 \\ 0 & 0 & 0 \end{bmatrix} \begin{bmatrix} \Delta\psi \\ \Delta\phi \\ \Delta\theta \end{bmatrix},
\tag{34}
$$

with the wheel radius r and the angular velocity $\omega = v/r$ of the wheel along the negative y-axis. From (34) we conclude that the system has a pure oscillatory motion in the yaw angle ψ and the roll angle ϕ with radial eigenfrequency ω. For the corresponding eigenmotion we will look at the path of the contact point C. The lateral displacement of the contact point Δy is kinematically coupled to the roll angle by $\Delta y = -r\Delta\phi$. The corresponding eigenmotion is the kinematic (or static) shimmy where the contact point C shows a sinusoidal path with wavelength $2\pi r$ and were the yaw angle and the roll angle are 90° out of phase.

To verify this result we made a finite element model where the fork has finite stiffness. The model consists of a three-dimensional wheel element [19] attached in point A to a flexible beam. The wheel has zero longitudinal slip, zero lateral slip, and zero spin. The inextensible beam which is compliant for bending in the
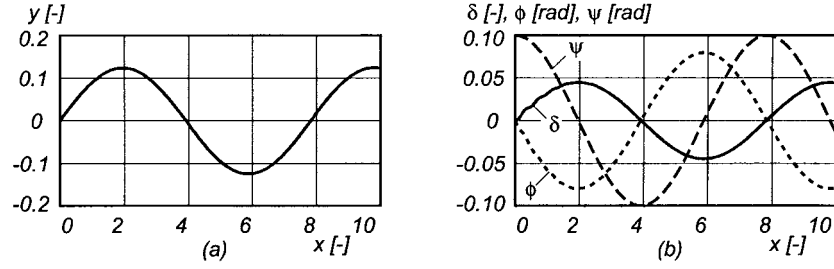
Figure 8. Kinematic shimmy motion; (a) the lateral contact point displacement y as a function of the longitudinal contact point displacement x and (b) the lateral beam deflection δ, the roll angle ϕ, and the yaw angle ψ of the wheel as a function of the longitudinal contact point displacement x.

yz-plane and rigid in the xz-plane is connected in B by a cylindrical hinge to the airplane. The hinge is free to rotate along its hinge axis and we release the radial deformation of the tire to make the problem statically determinate. We assume that the wheel has uniformly distributed unit mass and unit radius r. The massless beam has unit length l and a bending stiffness of $EI = 10$ with a relative damping of 1%. The caster wheel is moved forward at a unit speed v and the initial conditions are a yaw angle $\psi = 0.1$ [rad] and zero roll angle. Figure 8a shows the oscillatory path of the contact point, whereas in Figure 8b the lateral beam deflection δ, the roll angle ϕ and the yaw angle ψ of the wheel as a function of the longitudinal contact point displacement x are shown. A high frequency transient which dies out fast is just discernible in the lateral beam deflection δ and the roll angle ϕ, after which the system settles into periodic motion with constant amplitudes. We therefore truly can speak of a kinematic or static shimmy. The resulting wavelength is 7.83 which is about 25% longer than the previously found $2\pi r$ at unit radius r. It is expected that the wavelength increases since the wheel centre now can flex sideways. If we assume static loading then the beam is loaded by a shear force in A equal to the lateral contact force F_y and a moment in A which is equal to $F_y r$. The lateral beam deflection δ and the endpoint rotation ϕ which is in fact the roll angle of the wheel, are now coupled as in $\delta = -k\phi r$. The factor k is only a function of the ratio of the beam length over the wheel radius $\xi = l/r$ and can be calculated as $k = \xi(2\xi + 3)/(3\xi + 6)$. Reformulating the linearized dynamical equations (34) results in

$$\begin{bmatrix} \Delta\dot{\psi} \\ \Delta\dot{\phi} \\ \Delta\dot{\theta} \end{bmatrix} = \begin{bmatrix} 0 & \omega & 0 \\ -\frac{\omega}{1+k} & 0 & 0 \\ 0 & 0 & 0 \end{bmatrix} \begin{bmatrix} \Delta\psi \\ \Delta\phi \\ \Delta\theta \end{bmatrix}, \tag{35}$$

from which we conclude that the radial eigenfrequency of the kinematic shimmy is decreased by a factor $1/\sqrt{1+k}$, and the corresponding wavelength of the contact path is increased by a factor $\sqrt{1+k}$. In our case where $\xi = 1$ this results in a wavelength of 7.836 which compares well with the value from Figure 8.

4. Conclusion

A procedure has been described for formulating the dynamical equations of non-holonomic mechanical systems as well as their linearized equations. The procedure can be applied to systems with flexible bodies with the same ease as to systems with rigid bodies. Advantages of the procedure are the use of a set of minimal independent state variables, which avoid the use of differential-algebraic equations, and the analytic linearization, which is more accurate than numerical differentiation. The linearized equations can be used to analyse the stability of a nominal steady motion.

References

1. Lagrange, J.L., *Analytical Mechanics*, Kluwer, Dordrecht, 1997. (Original French first edition *Méchanique analitique*, Desaint, Paris, 1788.) (Translated from the French second edition *Mécanique analytique*, Courcier, Paris, 1811, by A. Boissonnade and V.N. Vagliente.)
2. Hertz, H., *Die Prinzipien der Mechanik in neuem Zusammenhange dargestellt*, Johann Ambrosius Barth, Leipzig, 1894.
3. Neĭmark, Ju.I. and Fufaev, N.A., *Dynamics of Nonholonomic Systems*, American Mathematical Society, Providence, RI, 1972. (Translated from the Russian edition, Nauka, Moscow, 1967.)
4. Kreuzer, E.J., 'Symbolische Berechnung der Bewegungsgleichungen von Mehrkörpersystemen', Dissertation, Fortschrittberichte der VDI Zeitschriften, Reihe 11, Nr. 32, 1979.
5. Nikravesh, P.E. and Haug, E.J., 'Generalized coordinate partitioning for analysis of mechanical systems with nonholonomic constraints', *ASME Journal of Mechanisms, Transmissions, and Automation in Design* **105**, 1983, 379–384.
6. Schwab, A.L. and Meijaard, J.P., 'Small vibrations superimposed on a prescribed rigid body motion', *Multibody System Dynamics* **8**, 2002, 29–49.
7. Besseling, J.F., 'The complete analogy between the matrix equations and the continuous field equations of structural analysis', in *International Symposium on Analogue and Digital Techniques Applied to Aeronautics: Proceedings*, Presses Académiques Européennes, Bruxelles, 1964, 223–242.
8. Van der Werff, K., 'Kinematic and dynamic analysis of mechanisms, A finite element approach', Dissertation, Delft University Press, Delft, 1977.
9. Jonker, J.B., 'A finite element dynamic analysis of flexible spatial mechanisms and manipulators', Dissertation, Delft University Press, Delft, 1988.
10. Cardona, A., Géradin, M. and Doan, D.B., 'Rigid and flexible joint modeling in multibody dynamics using finite-elements', *Computer Methods in Applied Mechanics and Engineering* **89**, 1991, 395–418.
11. Géradin, M. and Cardona, A., *Flexible Multibody Dynamics: A Finite Element Approach*, Wiley, Chichester, 2001.
12. Meijaard, J.P., 'Direct determination of periodic solutions of the dynamical equations of flexible mechanisms and manipulators', *International Journal for Numerical Methods in Engineering* **32**, 1991, 1691–1710.
13. Schwab, A.L., 'Dynamics of flexible multibody systems', Dissertation, Delft University of Technology, Delft, April 2002.
14. Jonker, J.B. and Meijaard, J.P., 'SPACAR – Computer program for dynamic analysis of flexible spatial mechanisms and manipulators', in *Multibody Systems Handbook*, W. Schiehlen (ed.), Springer-Verlag, Berlin, 1990, 123–143.
15. Whittaker, E.T., *A Treatise on the Analytical Dynamics of Particles and Rigid Bodies*, fourth edition, Cambridge University Press, Cambridge, U.K., 1937.

16. Bottema, O., 'On the small vibration of non-holonomic systems', *Proceedings Koninklijke Nederlandse Akademie van Wetenschappen* **52**, 1949, 848–850.
17. Den Hartog, J.P., *Mechanical Vibrations*, fourth edition, McGraw-Hill, New York, 1956.
18. Schwab, A.L. and Meijaard, J.P., 'The belt, gear, bearing and hinge as special finite elements for kinematic and dynamic analysis of mechanisms and machines', in Leinonen, T. (ed.), *Proceedings of the Tenth World Congress on the Theory of Machines and Mechanisms*, IFToMM, June 20–24, Oulu, Finland, Oulu University Press, 1999, Vol. 4, 1375–1386.
19. Schwab, A.L. and Meijaard, J.P., 'Dynamics of flexible multibody systems having rolling contact: Application of the wheel element to the dynamics of road vehicles', *Vehicle System Dynamics Supplement* **33**, 1999, 338–349.
20. Schwab, A.L. and Meijaard, J.P., 'Two special finite elements for modelling rolling contact in a multibody environment', in *Proceedings of the First Asian Conference on Multibody Dynamics*, ACMD'02, July 31–August 2, 2002, Iwaki, Fukushima, Japan, The Japan Society of Mechanical Engineering, 2002, 386–391.
21. Kantrowitz, A., 'Stability of castering wheels for aircraft landing gears', Technical Report 686, NACA, Washington DC, 1940, 147–162.